Glycolytic oscillations in single ischemic cardiomyocytes at near anoxia

Vladimir Ganitkevich, Violeta Mattea, and Klaus Benndorf

Department of Physiology II, University of Jena, D-07743 Jena, Germany

Previous studies have shown that oscillations of the metabolism can occur in cardiomyocytes under conditions simulating ischemia/reperfusion. It is not known whether they can also occur during real ischemia with near-anoxic oxygen tension. Here, using oxygen clamp in on-chip picochambers, we exposed single resting cardiomyocytes to near anoxia ($pO_2 < 0.1$ mm Hg). We show that at near anoxia, the mitochondrial membrane potential ($\Delta\Psi$) was kept by the F_1F_0-ATPase reversal, using glycolytic adenosine triphosphate (ATP). In many cells, activation of current through sarcolemmal K_{ATP} channels (I_{KATP}) started after a delay with one or several oscillations (frequency of 0.044 ± 0.002 Hz). These oscillations were time correlated with oscillations of $\Delta\Psi$. Metabolic oscillations at near anoxia are driven by glycolysis because (a) they were inhibited when glycolysis was blocked, (b) they persisted in cells treated with cytoplasmic reactive oxygen species scavengers, and (c) the highest rate of ATP synthesis during an oscillation cycle was associated with the generation of reducing equivalents. Glycolytic oscillations could be initiated upon rapid, but not slow, transition to near anoxia, indicating that the speed of ATP/ADP ratio drop is a determinant of their occurrence. At enhanced oxidative stress, the rate of ATP consumption was increased as indicated by rapid I_{KATP} activation with large-scale oscillations. These results show that metabolic oscillations occur in cardiomyocytes at near anoxia and are driven by glycolysis and modulated by mitochondria through the rate of ATP hydrolysis, which, in turn, can be accelerated by oxidative stress.

INTRODUCTION

When cardiomyocytes are exposed to substrate removal (O'Rourke et al., 1994; Romashko et al., 1998), chemical ischemia (Ryu et al., 2005; Yang et al., 2008), oxidative stress induced by glutathione depletion (Aon et al., 2007; Slodzinski et al., 2008), or photooxidation (Aon et al., 2003), metabolic oscillations are frequently observed. These oscillations are manifested either by cyclic depolarization of the mitochondrial membrane potential ($\Delta\Psi$) or cyclic changes of the cytoplasmic ATP/ADP ratio, which, in turn, is reflected by changes in I_{KATP} and cell excitability (O'Rourke et al., 1994; Aon et al., 2003; Ryu et al., 2005; Yang et al., 2008). Metabolic oscillations have been attributed to synchronization of the mitochondrial network of coupled oscillators by cytoplasmic reactive oxygen species (ROS) (Aon et al., 2006). The trigger for oscillations is thought to be oxidative stress due to radicals produced by laser flash–induced photooxidation (Zorov et al., 2000; Aon et al., 2003; Brady et al., 2004) that is supposed to simulate an elevated ROS production by the respiratory chain. During prolonged ischemia, various components of the respiratory chain involved in ROS production become damaged (Chen et al., 2008). ROS accumulation above some "critical" threshold is followed by a subsequent

ROS release into the cytosol through a postulated ROS-induced ROS release mechanism, involving the mitochondrial inner membrane anion channel (Aon et al., 2003) or the cyclosporine A–sensitive permeability transition pore (PTP) (Zorov et al., 2000; Brady et al., 2004).

Metabolic oscillations were also observed during chemical ischemia in cardiomyocytes with largely eliminated mitochondrial function, for example, when the mitochondrial "clamping" of ATP/ADP levels was prevented by blocking oxidative phosphorylation with cyanide and rotenone in the presence of a creatine kinase inhibitor (Ryu et al., 2005; Yang et al., 2008). Oscillations were not affected by cytoplasmic ROS scavengers. They were attributed to oscillatory glycolysis under conditions of ADP depletion in the phosphofructokinase reaction (Yang et al., 2008). Finally, the possibility of a cyclic activation of mitochondrial K_{ATP} channels has also been suggested (Ryu et al., 2005).

What all studies of metabolic oscillations in cardiomyocytes have in common is that they were performed at unrestricted access of atmospheric oxygen, e.g., with oxygen concentrations >10 times the physiological oxygen tension (Wilson et al., 1988; Rumsey et al., 1990; Gnaiger, 2001). Whether metabolic oscillations also occur at near anoxia is not known. However, the

The Rockefeller University Press $30.00
J. Gen. Physiol. Vol. 135 No. 4 307–319
www.jgp.org/cgi/doi/10.1085/jgp.200910332

307

oxygen tension is very important for evaluating the putative role of ROS in the genesis of metabolic oscillations. During ischemia, the oxygen in the affected tissue is consumed rapidly and the oxygen tension drops to near anoxia. Because the mitochondrial ROS production depends on both the degree of reduction of relevant electron carriers of the respiratory chain and the local oxygen availability (Turrens, 2003; Murphy, 2009), it can substantially vary in cardiomyocytes exposed to ischemia with near-anoxic oxygen tensions. ROS production is expected to be increased at more reduced states of the electron carriers in the respiratory chain (Murphy, 2009; Stowe and Camara, 2009), whereas a decreased oxygen availability should result in a decreased ROS production due to less substrate accepting electrons. Indeed, total ROS production of isolated mitochondria was reported to decrease under near anoxia (Turrens, 2003; Hoffman et al., 2007; Korge et al., 2008; Starkov, 2008), despite the fact that the proportion of electrons leaking to oxygen increases with slower respiration at lower oxygen tension (Hoffman and Brookes, 2009). Diminished ROS production at near anoxia most likely contributes to the result that the main ischemic injury happens upon reperfusion, when the oxygen availability is increased again and a burst of the ROS production occurs (Yellon and Hausenloy, 2007).

In this study, we used oxygen clamp in picochambers to address the question of whether or not metabolic oscillations appear in isolated cardiomyocytes exposed to near anoxia, and to specify the anticipated role of ROS in the genesis of these oscillations. We show that metabolic oscillations occur at near anoxia in ischemic cardiomyocytes at times when mitochondrial function is still preserved, i.e., during early ischemia, before $\Delta\Psi$ collapse and rigor develop. They are driven by glycolysis but could be affected by mitochondria through the changes in the rate of ATP hydrolysis leading to changes of ATP/ADP ratio. During early ischemia, at steady-state near anoxia ROS does not importantly contribute. However, under conditions favoring oxidative stress, cellular radical formation can contribute to this control by affecting the mitochondrial ATP hydrolysis rate and, hence, the ATP/ADP ratio. Glycolytic oscillations could be triggered by rapid, but not slow, transition to near anoxia, indicating that the rate of oxygen consumption in the ischemic heart can be a determinant of their occurrence.

MATERIALS AND METHODS

Preparation of mouse ventricular cardiomyocytes
Animals were housed and handled according to the guidelines of the German Animal Protection law, and the experiments were conducted in accordance with the Guide for the Care and Use of Laboratory Animals (1996. National Academy of Sciences, Washington, D.C.). Mouse ventricular cardiomyocytes were prepared as described previously (Ganitkevich et al., 2006).

Picochambers and experimental setup
The experimental setup was described in detail previously (Ganitkevich et al., 2006). In brief, picochambers were constructed on glass chips by coating one side with a 32-µm thick layer of a negative photoresist in which cuboid-like pits of 150-µm length, 40-µm width, and 32-µm depth were created, resulting in a geometric volume of 192 pL. The glass chips formed the bottom of the experimental chamber. In the headspace of the experimental chamber, an atmosphere of humidified argon was established to insulate the picochambers from the atmospheric air while having free access for glass pipettes. pO_2 in the solution of the picochamber could be controlled by setting the argon flow. When changing the argon flow rate, pO_2 at the cell could be changed rapidly in a step-like fashion (<5 s) in the range between <0.1 and 10 mm Hg, which is the critical range for control of oxidative metabolism (Wilson et al., 1988; Rumsey et al., 1990; Gnaiger, 2001). Hence, the argon flow rate defined the oxygen tension at the bottom of the experimental chamber. If not otherwise mentioned, the measurements were performed at the two argon flow rates of 30 and 100 ml/min. With an argon flow rate of 30 ml/min, the pO_2 at the bottom of the chamber was 10 mm Hg, as measured with either a Clark electrode or Pt-porphyrin quenching (MFPF-100-1 with FOSPOR-R sensor; Ocean Optics). With an argon flow rate progressively higher, the pO_2 levels became, respectively, lower (Fig. S1 A). Because below pO_2 = 2 mm Hg the Clark electrode became progressively erroneous, the pO_2 at the argon flow rate of 100 ml/min was preferably measured by Pt-porphyrin quenching, resulting in a value between 0.04 and 0.10 mm Hg. The value of 0.04 mm Hg was obtained as follows. A further increase of the argon flow rate to 200 ml/min led to a further slowing of the phosphorescence lifetime, indicating a further decrease of pO_2 (Fig. S1 B), whereas no further increase of the lifetime was observed when the sensor was exposed to 100% nitrogen outside the setup. This indicates that any further reduction of pO_2 was below the resolution of the sensor of 0.04 mm Hg. Hence, with an argon flow rate of 100 ml/min, the cardiomyocyte in a picochamber was exposed to pO_2 between 0.04 and 0.1 mm Hg. Routinely, pO_2 was monitored with the Clark electrode because the measurement with Pt-porphyrin could interfere with the fluorescence measurement of $\Delta\Psi$. We conclude that changing the argon flow rate between 30 and 100 ml/min varied the oxygen tension at the cell between 10 and <0.1 mm Hg, respectively. Rapid (5 s) and slow (minutes) changes of pO_2 were achieved by applying step and ramp voltages to the flow controller (Smart-Track-100; Sierra Instruments).

Patch clamp technique
Transmembrane currents of cardiomyocytes were recorded with the patch clamp technique in the whole cell configuration as described previously (Ganitkevich et al., 2006). If not otherwise noted, the holding potential was −80 mV and the cells were depolarized to +40 mV for 100 ms at 2 Hz. All experiments were performed at room temperature (22 ± 1°C).

Fluorescence optical measurements
$\Delta\Psi$ was measured optically (Ganitkevich et al., 2006) by using the fluorescence dye tetramethylrhodamine methyl (or ethyl) ester (TMRM or TMRE). Most experiments were performed in the de-quench mode (Nicholls and Ward, 2000; Duchen et al., 2003). The cells were incubated with a KB solution containing 2 µM of either TMRM or TMRE at room temperature for 15 min. Under the experimental conditions used, the two dyes provided indistinguishable results. For most experiments, TMRM was used in the de-quench mode, which provided two advantages. First, the

sensitivity is ~100 times higher compared with the nonquenching mode (Voronina et al., 2004). Second, because the photomultiplier (PMT) signal was collected from the whole picochamber, where all dye was trapped, the diffusional loss via the pipette was only minimal, avoiding redistribution problems with the dye, as present in experiments with large solution volumes (Nicholls and Ward, 2000). However, because of concerns about a high matrix concentration of the dye, some control experiments were done with low nanomolar concentrations. For these experiments in the nonquench mode, the cells were incubated in Tyrode's solution containing 20 nM TMRM for 15 min and imaged every 5 s with an Apotome microscope (Carl Zeiss, Inc.). "Pseudoconfocal" images were processed with the ImageJ software (National Institutes of Health). To avoid bleaching of the dye in long-lasting experiments, the development of rigor was accelerated by the inclusion of low concentrations (50 or 100 nM) of the uncoupler FCCP in the patch pipette solution. To estimate the cytosolic [ATP], free [Mg^{2+}] was measured with MgGreen as described previously (Leyssens et al., 1996). The cells were loaded with 5 µM MgGreen-AM for 30 min. 2′,7′-dichlorodihydrofluorescein (H_2DCF) oxidation was measured as described previously (Ganitkevich et al., 2006). Cells were loaded with 5 µM CM-H_2DCFDA for 20 min. NAD(P)H fluorescence could not be measured in these experiments because UV illumination destroyed the photoresist used for chip production. Flavoprotein fluorescence signals were too small to be usable as metabolic parameter during metabolic oscillations.

Data acquisition and analysis
Measurements were controlled and data were collected and analyzed with the ISO2/ISO3 software and hardware (12-bit resolution; MFK) running on a PC. The sampling rate was 1 kHz. The results are presented as mean ± SE.

Chemicals and solutions
All chemicals were of analytical grade. Tyrode's solution contained (in mM): 140 NaCl, 5.4 KCl, 1.2 $CaCl_2$, 0.5 $MgCl_2$, 0 glucose, and 10 HEPES, pH 7.4 (NaOH). Intracellular solution in the patch pipette contained (in mM): 140 KCl, 10 HEPES, and 5 EGTA, pH 7.3 (KOH). The cells were stored for experimental use in KB medium containing (in mM): 30 KCl, 30 KH_2PO_4, 50 glutamine acid, 20 taurine, 20 HEPES, 10 glucose, 3 $MgSO_4$, and 0.5 EGTA, pH 7.3 (KOH). Drugs were applied by flooding the picochamber with the appropriate solution. Normally, the PMT was switched off during solution exchanges to avoid the recording of artifacts. Recording was continued after the solution surrounding the cardiomyocyte was reduced to the picochamber volume again.

Online supplemental material
Fig. S1 shows the dependence of pO_2 at the bottom of the experimental chamber on the rate of Ar flow. Oxygen quenching of Pt-porphyrin luminescence (FOSPOR-R sensor with MFPF-100-1; Ocean Optics) was measured at different Ar flow rates. Fig. S2 demonstrates that glycolytic ATP is required to sustain ΔΨ and to keep K_{ATP} channels closed at near anoxia. Glycolysis was impaired with iodoacetic acid (IAA) or 2-deoxyglucose (2-DG), whereas oligomycin or bongkrekic acid (BKA) was used to inhibit the F_1F_0-ATPase. The online supplemental material is available at http://www.jgp.org/cgi/content/full/jgp.200910332/DC1.

RESULTS

ΔΨ is maintained during I_{KATP} activation in resting cardiomyocytes exposed to near anoxia
Resting cardiomyocytes (5 mM EGTA in the patch pipette) responded to a change from atmospheric pO_2

(160 mm Hg) to near anoxia ($pO_2 < 0.1$ mm Hg) with only small depolarization of ΔΨ, which was regularly <10% of the signal obtained with the uncoupler FCCP (Fig. 1 A). After a variable delay (usually 5–10 min), I_{KATP} became activated, suggesting that the cytoplasmic ATP/ADP ratio could not be maintained. This was confirmed by measurements of the cytosolic [Mg^{2+}] with MgGreen. At near anoxia, the free [Mg^{2+}] became increased when I_{KATP} was activated. Time courses of I_{KATP} and MgGreen signal dissociated, which is likely due to a progressive decrease of pH at near anoxia (Ganitkevich et al., 2006), affecting fluorescence properties of the indicator. Reoxygenation, which restored ATP synthesis by oxidative phosphorylation, rapidly removed I_{KATP} and decreased the [Mg^{2+}] ($n = 6$; Fig. 1 B). Most notably, ΔΨ was kept largely polarized under conditions when the cytosolic [ATP] significantly dropped, as indicated by the activation of I_{KATP} (Fig. 1 A). However, in the de-quench mode, the relation of the TMRM fluorescence signal to ΔΨ is presumably not simple. We therefore performed experiments in the nonquench mode, in which the fluorescence signals are likely to be more directly related to ΔΨ (Duchen et al., 2003). Activation of I_{KATP} at near anoxia was not associated with a measurable signal (Fig. 1 C) until rigor contracture occurred and ΔΨ collapsed ($n = 9$). Notably, the mitochondria located under the patch pipette kept some ΔΨ, most likely due to an oxygen leak from the patch pipette and accumulated dye that was released from more remote mitochondria where ΔΨ collapsed. This shows that any residual ATP production by these mitochondria did not prevent development of the rigor contracture (Fig. 1 C).

To prove that glycolytic ATP is needed for keeping ΔΨ polarized at near anoxia, glycolysis was manipulated. The glycolytic ATP production was either inhibited by IAA or the cytoplasmic ATP consumption was accelerated by 2-DG. In the presence of IAA, ΔΨ was sustained at $pO_2 = 10$ mm Hg, but rapidly and almost completely collapsed at near anoxia (Fig. S2 A). The results with 2-DG were similar to those obtained with IAA (Fig. S2 B).

To prove that the reversal of the F_1F_0-ATPase keeps ΔΨ at near anoxia at the expense of glycolytic ATP, cells were treated with oligomycin. In the presence of oligomycin, I_{KATP} appeared not only at near anoxia, but after a delay also at $pO_2 = 10$ mm Hg, suggesting that ATP synthesis was inhibited. At the same time, ΔΨ was largely sustained because of an intact respiratory chain. After activation of I_{KATP}, stepping to near anoxia led to the collapse of ΔΨ (Fig. S2 C). Finally, the adenine nucleotide translocator (ANT) inhibitor BKA was applied to diminish ATP hydrolysis by the F_1F_0-ATPase (Nicholls and Ferguson, 2002). In the presence of BKA, the ability of the cell to sustain ΔΨ at near anoxia became progressively reduced (Fig. S2 D).

Collectively, these results show that the activation of I_{KATP} indicates a progressive imbalance between glycolytic ATP

synthesis and hydrolysis of ATP by the reverse action of the F_1F_0-ATPase.

At near anoxia, oscillations of I_{KATP} and $\Delta\Psi$ occur conjointly
Activation of I_{KATP} started in many cells (34% of 198) with one or more oscillations (Fig. 2 A). They occurred always at the beginning of I_{KATP} activation, ceased when the current activated further, were paralleled by small oscillations of $\Delta\Psi$, and had a frequency of 0.044 ± 0.002 Hz ($n = 37$). I_{KATP} oscillations also occurred in cells not loaded with TMRM ($n = 8$; Fig. 2 B). Comparison of the time courses of I_{KATP} and $\Delta\Psi$ during oscillations revealed an intimate temporal correlation (Fig. 2, C and D). Because at near anoxia both I_{KATP} and $\Delta\Psi$ are linked to the cytoplasmic ATP/ADP ratio, these results suggest that the cytoplasmic

ATP/ADP ratio oscillates, resulting in oscillations of both I_{KATP} and the ability of the F_1F_0-ATPase to keep $\Delta\Psi$. These results also suggest that in resting cardiomyocytes with an intact creatine kinase system, no significant spatial gradients in the ATP/ADP ratio were present at the time scale of metabolic oscillations.

ROS scavengers and modulators of the inner mitochondrial membrane conductance do not prevent metabolic oscillations
Only low ROS levels are expected at near anoxia. To test an involvement of ROS in the control of metabolic oscillations, cells were pretreated with redox-active compounds. Oscillatory behavior of I_{KATP} and $\Delta\Psi$ was still observed in cells preloaded with various cytoplasmic ROS scavengers or superoxide dismutase mimetics like TEMPOL,
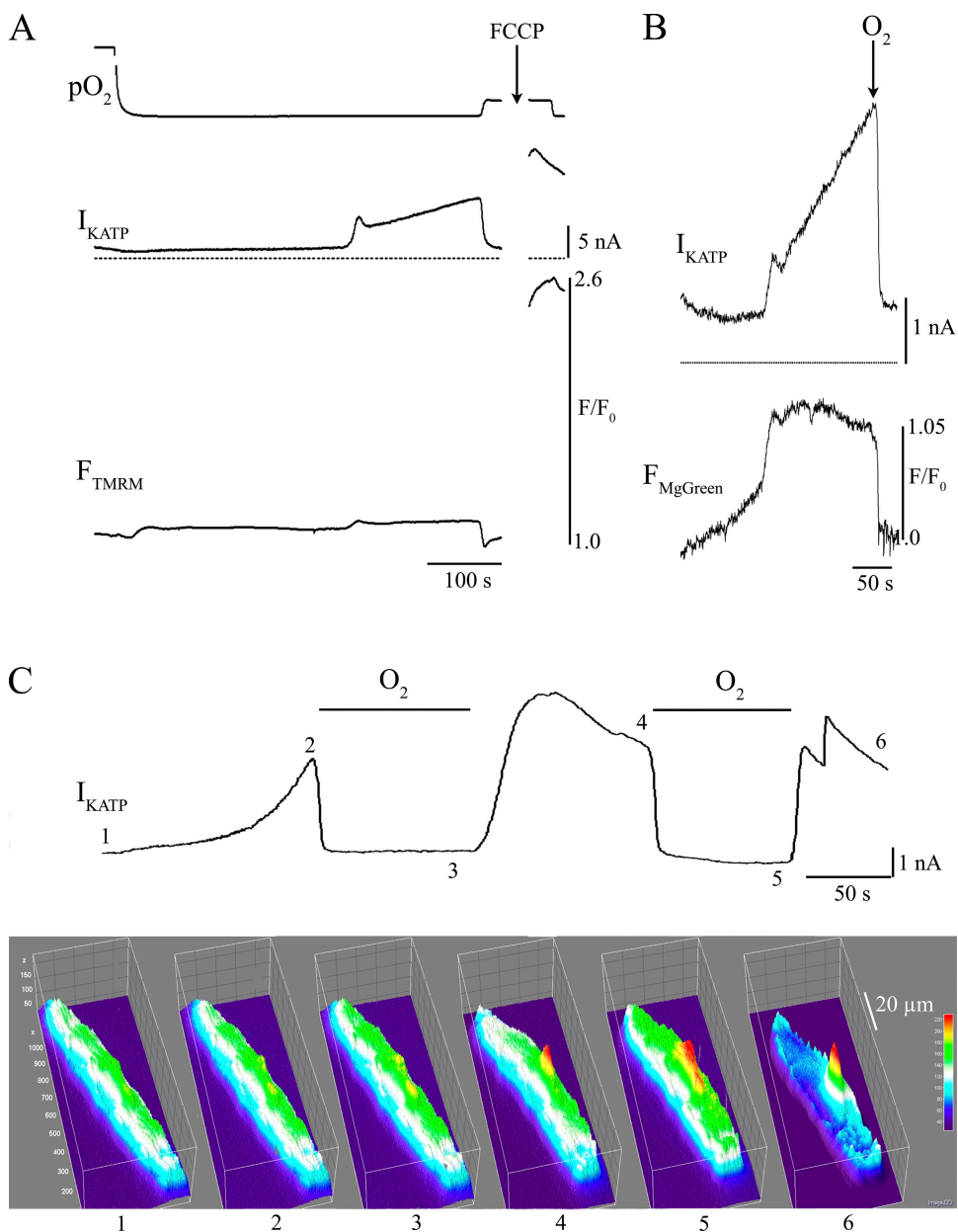

Figure 1. Changes in I_{KATP} and $\Delta\Psi$ in single cardiomyocytes subjected to near anoxia. (A) I_{KATP} activation was generally measured at +40 mV, and $\Delta\Psi$ depolarization was monitored by TMRM fluorescence after a decrease of pO_2 from 160 to <0.1 mm Hg. The response shown is representative of >200 cells. Reoxygenation to 10 mm Hg removed I_{KATP} and restored $\Delta\Psi$. The uncoupler FCCP (5 µM) was used in all experiments as a reference for both maximal I_{KATP} activation and $\Delta\Psi$ depolarization. (B) Simultaneous measurement of I_{KATP} activation and MgGreen fluorescence at near anoxia. The increase in $F_{MgGreen}$ indicates an elevation of $[Mg^{2+}]$ due to a fall of ATP ($n = 6$). Reoxygenation restored ATP synthesis, and K_{ATP} channels were rapidly closed. (C) Activation of I_{KATP} at near anoxia in a cell loaded with a low concentration of TMRM (20 nM; $n = 9$). I_{KATP} activation was favored by the presence of 50 nM FCCP in the patch pipette solution. Reoxygenation intervals removed I_{KATP}. At the time points indicated by numbers, "pseudo-confocal" images were acquired (bottom). A detectable change in the TMRM signal was observed only after rigor contracture developed.

N-(2-mercaptopropionyl)-glycine (MPG), 3-methyl-1-phenyl-2-pyrazolin-5-one (MCI-186), and Mn(III)-tetrakis-(4-benzoic-acid)-porphyrin (MnTBAP; all 5 mM; ≥60-min pretreatment; mean frequency 0.039 ± 0.003 Hz; $n = 22$). Hence, at near anoxia, ROS are not likely to contribute significantly to metabolic oscillations.

To test for an involvement of mitochondrial K_{ATP} channel and PTP, appropriate ligands were used. Metabolic oscillations persisted in cells pretreated with 100 µM diazoxide (mitoK_{ATP} channel opener), 100 µM 5-hydroxy-decanoate (5-HD; mitoK_{ATP} channel blocker), or 1 µM cyclosporine A (PTP blocker; mean frequency 0.035 ± 0.002 Hz; $n = 12$). These findings make the involvement of mitoK_{ATP} channels and the PTP in the control of metabolic oscillations at this early stage of ischemia unlikely.

Anion channel blockers (4,4'-diisothiocyanostilbene-2,2'-disulfonic acid [DIDS] and 4´-chlorodiazepam), which were previously shown to reduce reperfusion injury (Akar et al., 2005), induced a rapid and complete collapse of $\Delta\Psi$ at near anoxia (unpublished data), consistent with reports that inhibition of voltage-dependent anion-selective channel and/or ANT inhibits the ATP transport into the mitochondrial matrix, preventing ATP hydrolysis by the F_1F_0-ATPase required to keep $\Delta\Psi$ (Báthori et al., 2006).

The results so far show that metabolic oscillations do occur in cardiomyocytes at near anoxia, and they suggest that glycolysis is the key player. They do not reveal, however, whether and how mitochondria are involved.

Mitochondrial state affects metabolic oscillations at near anoxia

To gain further insight into the mechanisms underlying the metabolic oscillations at near anoxia, the development of I_{KATP} was interrupted by short (30-s) intervals of reoxygenation (pO_2 = 10 mm Hg). Reoxygenation allows the cells to respire, hyperpolarize $\Delta\Psi$, and produce ATP by oxidative phosphorylation, thus "clamping"
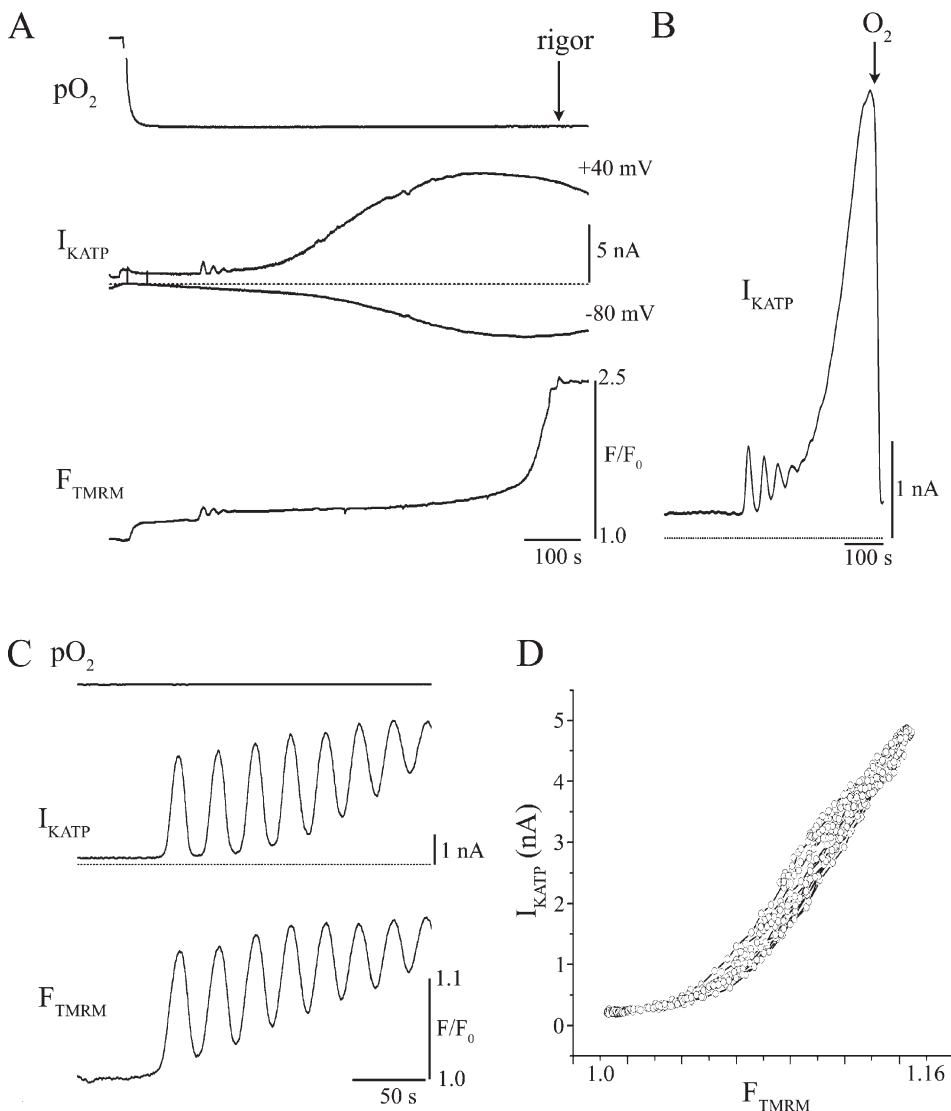

Figure 2. Oscillations of I_{KATP} and $\Delta\Psi$ in cardiomyocytes at near anoxia. (A) Transition to near anoxia is followed by oscillations of both I_{KATP} and $\Delta\Psi$ at +40 mV, but not at the holding potential (−80 mV). Oscillations were observed in 67 cells. (B) Similar current oscillations were recorded in cells not loaded with TMRM ($n = 8$). (C) Simultaneous recording of I_{KATP} and $\Delta\Psi$ at near anoxia, demonstrating that the oscillations were in phase. (D) Temporal correlation between I_{KATP} and $\Delta\Psi$ during the oscillations shown in C. All transitions to near anoxia were from 160 to <0.1 mm Hg.

the ATP/ADP ratio to a high level. Return to near anoxia again inhibits respiration and depolarizes $\Delta\Psi$, but at a higher ATP/ADP level, because ATP is produced during the preceding reoxygenation interval.

Most notably, shortly after a rapid (5-s) return to near anoxia, I_{KATP} rapidly activated, and to a higher level than before reoxygenation, despite some ATP that must have been synthesized during the preceding reoxygenation interval (Fig. 3 A). Moreover, when the protocol was applied shortly before measurable I_{KATP} activation, a burst of I_{KATP} was recorded (Fig. 3 B). Repetitive application of this protocol during activation of I_{KATP} induced progressively larger bursts of I_{KATP}, which switched over to oscillations (Fig. 3 B). When $\Delta\Psi$ was recorded together with I_{KATP}, the I_{KATP} burst was paralleled by a transient depolarization of $\Delta\Psi$ (Fig. 3 C). The conjoint oscillations of both $\Delta\Psi$ and I_{KATP} could be evoked (Fig. 3 D, after first reoxygenation interval) or, if already present, potentiated (Fig. 3 D, after second reoxygenation interval) by a rapid return to near anoxia. ROS scavengers did not prevent potentiation effects of reoxygenation intervals (unpublished data).

These results suggest that shortly after a rapid return to near anoxia after a reoxygenation interval, the
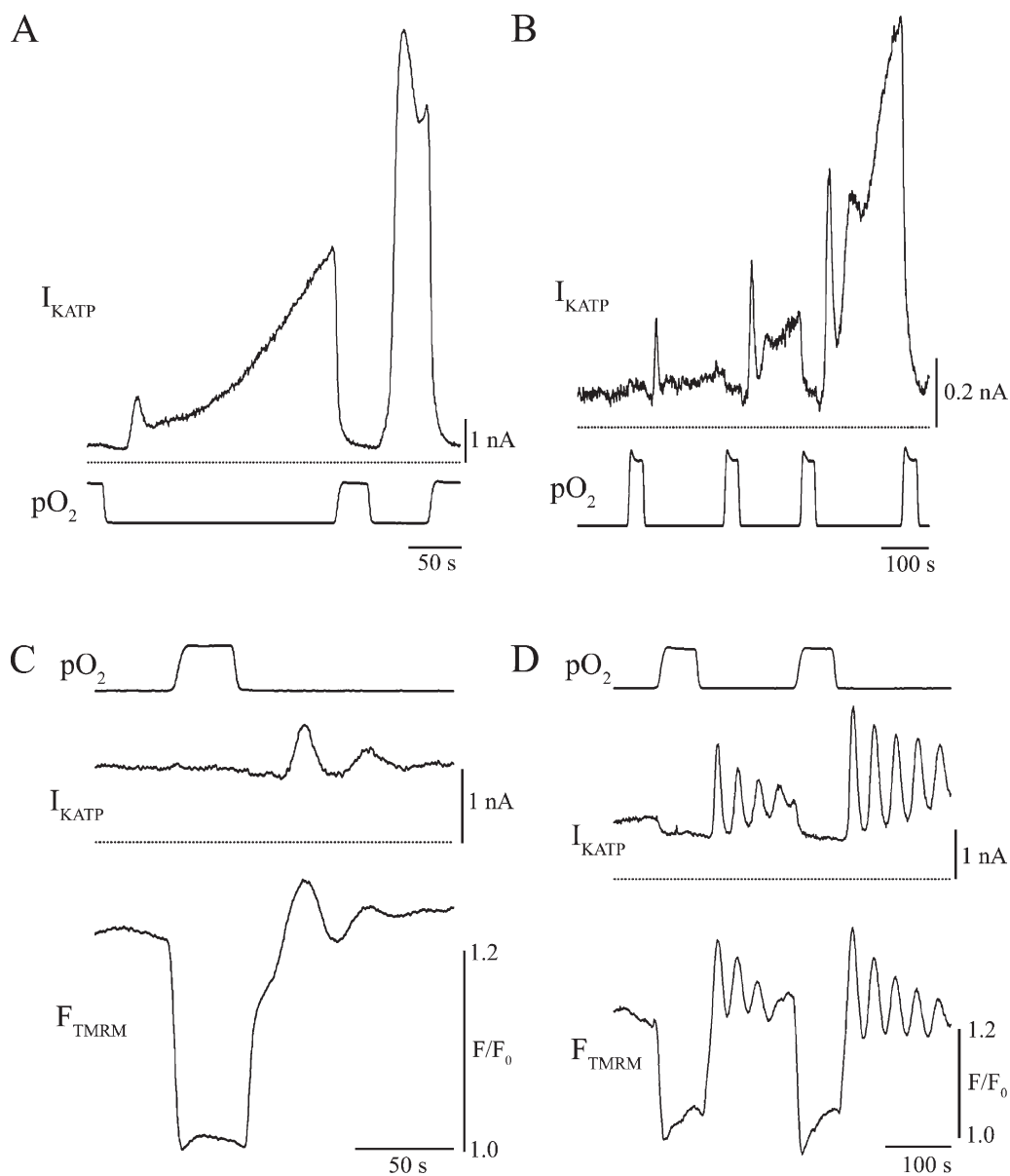

Figure 3. I_{KATP} and its oscillations are potentiated after rapid transition to near anoxia. (A) I_{KATP} activated slowly at near anoxia, but rapidly and to higher amplitude after a short reoxygenation interval. (B) Progressive potentiation and initiation of oscillations of I_{KATP} at near anoxia after repetitive reoxygenation intervals. (C) Potentiation of I_{KATP} at near anoxia after a reoxygenation interval is paralleled by a transient $\Delta\Psi$ depolarization. (D) Initiation and potentiation of oscillatory behavior of both I_{KATP} and $\Delta\Psi$ after a first and second reoxygenation interval, respectively. All reoxygenation intervals were from <0.1 to 10 mm Hg and had a duration of 30 s.

hydrolysis of ATP transiently increases. Because the effect was not sensitive to ROS scavengers, we hypothesize that it could be due to a switch of the F_1F_0-ATPase from ATP synthesis to ATP hydrolysis as the result of rapid mitochondrial depolarization.

$\Delta\Psi$ is a determinant of the ATP hydrolysis rate at near anoxia

To prove that $\Delta\Psi$ determines the ATP hydrolysis rate by the F_1F_0-ATPase, glycolysis was blocked by 1 mM IAA and the F_1F_0-ATPase was reversed by near anoxia, leading to cytoplasmic ATP consumption until the development of rigor and collapse of $\Delta\Psi$. As in cells with intact glycolysis (Fig. 2 A), $\Delta\Psi$ was depolarized only slightly upon transition to near anoxia (Fig. 4 A). Within less than a minute, however, I_{KATP} was completely activated and $\Delta\Psi$ collapsed ($n = 5$), suggesting that with glycolytic ATP supply blocked, ATP was rapidly consumed by the F_1F_0-ATPase (compare Fig. 2 A). Reoxygenation restored $\Delta\Psi$ and removed I_{KATP} after a delay, when oxidative phosphorylation had produced enough ATP (Fig. 4 A). This shows that the respiratory chain was still functional. Notably, at near anoxia, $\Delta\Psi$ became depolarized at an increasingly higher rate with a maximum close to time of complete activation of I_{KATP} (Fig. 4 A). Hence, depolarized mitochondria reduce the ATP/ADP ratio at a higher rate. The rate of $\Delta\Psi$ depolarization decreased again when the ATP/ADP ratio fell further, as indicated by the collapse of $\Delta\Psi$ and the development of rigor. Reoxygenation restored $\Delta\Psi$, indicating that at this time, the respiratory chain is not significantly damaged (Fig. 4 A). At blocked glycolysis, metabolic oscillations were never observed ($n = 5$).

To directly demonstrate that the rate of ATP hydrolysis by mitochondria affects metabolic oscillations, we applied a low concentration of an uncoupler FCCP to cells with intact glycolysis to reduce $\Delta\Psi$ kept at near anoxia and thus to accelerate ATP hydrolysis by the F_1F_0-ATPase.

In the presence of 20 nM FCCP, transition to near anoxia induced large depolarization of $\Delta\Psi$ and an immediate maximal activation of I_{KATP} with large-scale oscillations ($n = 12$; Fig. 4 B). Similar to cells not treated with an uncoupler, these oscillations of I_{KATP} were potentiated after intervals of reoxygenation (Fig. 4 B). However, the amplitude of I_{KATP} oscillations was much larger compared with that usually recorded in untreated cells (Figs. 2 and 3). Oscillations of I_{KATP} were also paralleled by oscillations of $\Delta\Psi$, until its collapse due to the fall of the ATP/ADP ratio. Nevertheless, the respiratory chain was still able to polarize $\Delta\Psi$ upon reoxygenation (Fig. 4 B).

These results further confirm the finding that glycolysis is responsible for metabolic oscillations at near anoxia, that mitochondria are suppliers of ADP for the phosphofructokinase, and that this supply depends on $\Delta\Psi$ kept at near-anoxic conditions. Moreover, because $\Delta\Psi$ is a determinant of the ATP hydrolysis rate, the speed of the fall of the ATP/ADP ratio should also depend on the rate of $\Delta\Psi$ depolarization. This could be verified experimentally.

The rate of oxygen drop determines mitochondrial influence on metabolic oscillations

We induced both a rapid (5-s) and a slow drop of oxygen to near anoxia in the same experiment. With the rapid drop, oscillations of both I_{KATP} and $\Delta\Psi$ were observed (Fig. 5 A; $n = 5$). Reoxygenation restored
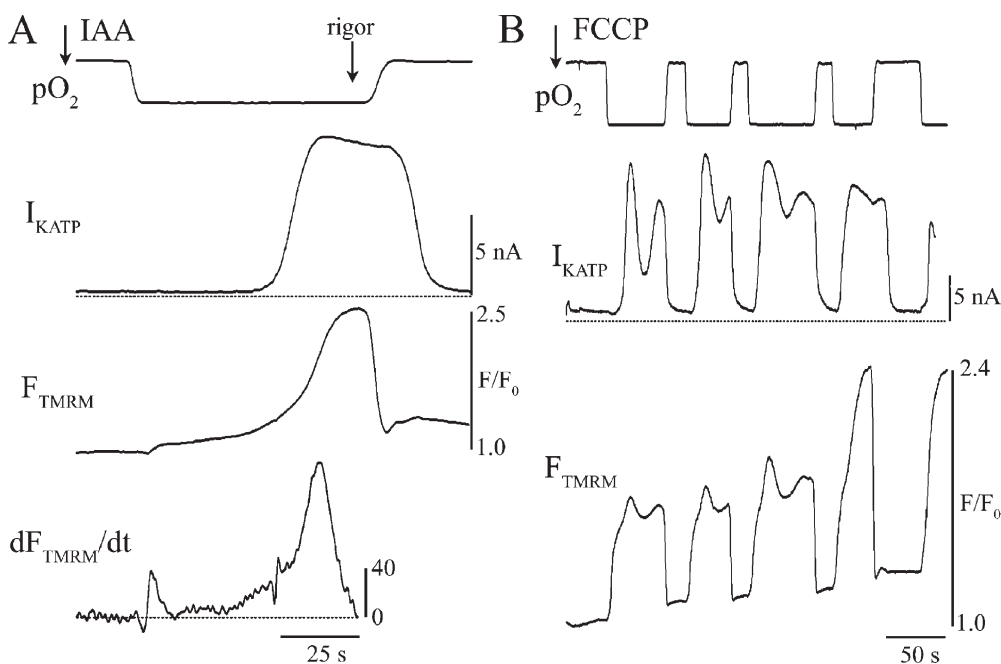

Figure 4. $\Delta\Psi$ is a determinant of the ATP hydrolysis rate. (A) With glycolysis blocked by 1 mM IAA, I_{KATP} activation and $\Delta\Psi$ depolarization occurred without oscillations. The rate of $\Delta\Psi$ depolarization was progressively increased until rigor developed ($n=5$). (B) Partial mitochondrial uncoupling with 20 nM FCCP resulted in a large $\Delta\Psi$ depolarization at near anoxia and initiation of large-scale I_{KATP} oscillations ($n = 12$).

ΔΨ and removed I_{KATP}. When the pO_2 was reduced slowly to near anoxia within 2 min, I_{KATP} was activated again and ΔΨ depolarized at a slower rate, but oscillations of ΔΨ and I_{KATP} were largely absent (Fig. 5 A). Similar results were obtained when protocols were applied in the opposite order ($n = 5$). Similarly, a stepwise reduction of pO_2 to near anoxia within 3 min depolarized ΔΨ and activated I_{KATP} without inducing oscillations ($n = 5$; Fig. 5 B). Reoxygenation restored ΔΨ and abolished I_{KATP}; subsequent rapid transition to near anoxia again evoked oscillations of both I_{KATP} and ΔΨ.

These results suggest that the speed of transition to near anoxia, i.e., the rate of ΔΨ depolarization and fall of the ATP/ADP ratio is an important factor for the genesis of glycolytic oscillations.

Oxidative stress modulates metabolic oscillations

We found no role of ROS at near anoxia, as expected with little ROS production at a very low pO_2. This conclusion is based on the failure of scavengers to prevent metabolic oscillations. Instead, all results are in support of the idea that glycolysis is a critical determinant of the metabolic oscillations. Nevertheless, ROS might be important under conditions of myocardial ischemia because they are expected to be produced during reperfusion, causing damage of the respiratory chain. We therefore studied whether and how cellular ROS production affects metabolic oscillations. Doing this, we were aware that measurement of ROS in cells is a challenging task because no really suitable tools are available (Dikalov et al., 2007; Wardman, 2007). Commonly used H_2DCF is oxidized in the cell to the fluorescent compound DCF, and the increase of green fluorescence is used as an indicator of ROS production. However, it was shown in several insightful studies that upon illumination, DCF could act as photosensitizer for oxidation of cellular reductants (reduced glutathione [GSH] and NADH), thus producing radicals itself (Marchesi et al., 1999; Rota et al., 1999a,b). Subsequent electron transfer from these radicals to molecular oxygen produces superoxide (Bonini et al., 2006; O'Neill and Wardman, 2009). Moreover, as DCF is a two-electron oxidation product of H_2DCF, an intermediate radical is formed during oxidation, which reacts with oxygen to produce superoxide directly (Bonini et al., 2006; Wardman, 2007; Wrona et al., 2008). Therefore, DCF itself induces oxidative stress in a self-amplifying oxygen-consuming chain reaction, which depends on light, oxygen concentration, and the redox status of the cell (Wardman, 2007). We used these properties of DCF, in combination with substances having well-established effects on mitochondrial ROS production, to assess how different degrees of oxidative stress affect metabolic oscillations, reflected by I_{KATP}.

Because in an experiment the DCF fluorescence continuously increased upon illumination, as expected for a self-amplifying chain reaction, we used the rate of fluorescence increase (dF_{DCF}/dt) as the measure of oxidative stress (Fig. 6).

When the cells were treated with the complex III Q_o site inhibitor stigmatellin (1 µM; $n = 7$), which blocks ROS production (Nicholls and Ferguson, 2002; Turrens, 2003), the rate of H_2DCF oxidation increased only very slowly and I_{KATP} became activated slowly and showed oscillatory behavior (Fig. 6 A). This result suggests that blocking mitochondrial ROS production at complex III did not prevent glycolytic oscillations.
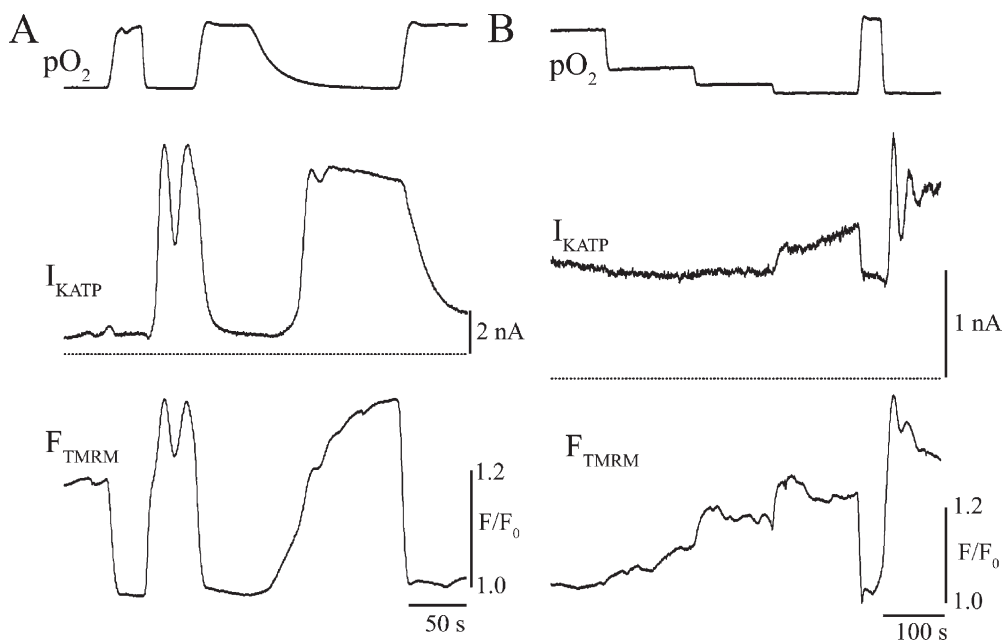

Figure 5. The rate of oxygen drop to near anoxia is a determinant for the oscillatory behavior of both I_{KATP} and ΔΨ. (A) I_{KATP} and ΔΨ oscillations occurred after a rapid (5-s) transition to near anoxia, but were largely absent when conditions at near anoxia were reached slowly (2 min; $n = 5$). During reoxygenation the oxygen tension was 10 mm Hg. (B) Stepwise transition to near anoxia within 3 min activated I_{KATP} and depolarized ΔΨ without oscillations, whereas the next fast transition triggered oscillatory behavior of both signals ($n = 5$). pO_2 was changed between 10 and <0.1 mm Hg.

When cells were treated with the complex III Q_i site inhibitor antimycin (1 µM; $n = 5$), which is known to greatly enhance ROS production by the respiratory chain (Nicholls and Ferguson, 2002; Turrens, 2003; Starkov, 2008), the rate of H_2DCF oxidation increased rapidly and continuously (Fig. 6 B). I_{KATP} activated much faster compared with the activation in the presence of stigmatellin and showed oscillatory behavior. Rapid transition from $pO_2 = 10$ mm Hg to near anoxia induced a transient increase of the H_2DCF oxidation rate lasting ~20 s (Fig. 6 B). It was shown before that this acceleration of H_2DCF oxidation is due to an electron transfer from thiyl radicals formed during preceding oxidative stress, which was suppressed in the presence of oxygen (Korge et al., 2008; Wrona et al., 2008). This is supported by the result that transient acceleration of H_2DCF oxidation was nearly absent with stigmatellin

with mitochondrial ROS production blocked, indicating a much lower degree of oxidative stress in the presence of stigmatellin.

When the cells were treated with the complex I inhibitor rotenone (1 µM; $n = 5$), which facilitates the ROS production at the FMN site of this complex (Nicholls and Ferguson, 2002; Turrens, 2003; Starkov, 2008), the rate of H_2DCF oxidation increased continuously, and an H_2DCF oxidation burst similar to that observed with antimycin was seen upon transition to near anoxia (Fig. 6 C). I_{KATP} activated quickly and showed oscillatory behavior. The degree of oxidative stress, estimated from the rate of the H_2DCF oxidation at $pO_2 = 10$ mm Hg after the addition of the blocker, was highest with antimycin, followed by rotenone. The results with stigmatellin were not significantly different from control (Fig. 6 D).
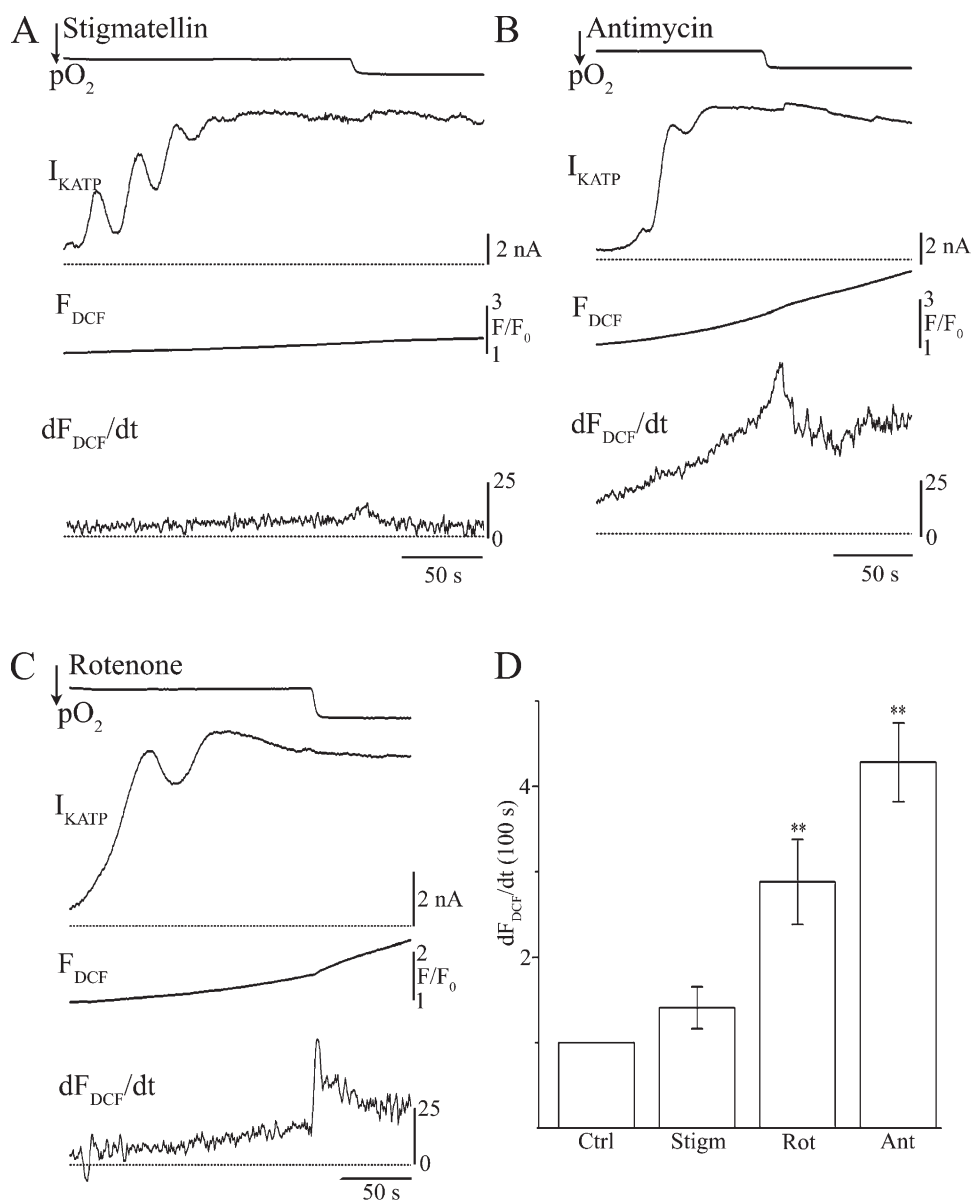

Figure 6. Activation of I_{KATP} in cardiomyocytes exposed to oxidative stress. Simultaneous recording of I_{KATP} activation and H_2DCF oxidation in cardiomyocytes treated with either (A) 1 µM stigmatellin ($n = 7$), (B) 1 µM antimycin ($n = 5$), or (C) 1 µM rotenone ($n = 7$). Transitions from pO_2 of 10 to <0.1 mm Hg induced H_2DCF oxidation by thiyl radicals. (D) Quantification of the degree of oxidative stress. Normalized values of the rate of the rise of DCF fluorescence 100 s after the addition of drugs. The oxidation rate of H_2DCF with both antimycin (Ant) and rotenone (Rot) was significantly different from control (Ctrl), whereas it was not significantly changed with stigmatellin (Stigm).

Collectively, our experiments demonstrate that elevated ROS levels are not necessary for the oscillatory behavior of I_{KATP}, through enhanced radical formation results in a faster fall of the ATP/ADP ratio, i.e., in an acceleration of ATP hydrolysis. Our results also demonstrate the problems of using DCF within cells. Thiyl (as well as other) radicals use oxygen as an electron sink to form superoxide, which is then dismutated in its usual way (Winterbourn, 1993, 2008; Winterbourn and Hampton, 2008), so that the lowering of pO_2 results in a redistribution of unpaired electrons between other acceptors. Therefore, interpretation of DCF fluorescence signals from cells is difficult, especially when pO_2 is varied. We therefore restricted our measurements with DCF to a constant low pO_2 of <0.1 mm Hg. We aimed to relate changes of the ATP/ADP ratio, reflected by I_{KATP} to the cellular redox state, during metabolic oscillations at near anoxia.

Oscillations of the H_2DCF oxidation rate and I_{KATP} at near anoxia are closely time related

At near anoxia, little superoxide is produced (Turrens, 2003; Korge et al., 2008; Muller, 2009). In the absence of oxygen, H_2DCF oxidation arises from thiyl radicals (Korge et al., 2008; Wrona et al., 2008) formed by photoreduction of DCF (Marchesi et al., 1999). Like other fluorescent dyes, DCF is activated by visible light to a triplet state that is reactive toward reducing agents like GSH, generating thiyl radicals (Marchesi et al., 1999). Notably, NAD(P)H can substitute for GSH and photoreduce the dye even much faster (Marchesi et al., 1999). Because we could not measure NAD(P)H fluorescence directly (see Materials and methods), we used this peculiarity of DCF to compare I_{KATP} and the H_2DCF oxidation rate, which should be related to [NAD(P)H] and hence to the cellular redox state. Because the glycolytic ATP flux is accompanied with the production of NAD(P)H, we could assume that that oscillations of the ATP/ADP ratio are also reflected by DCF fluorescence.

Upon transition to near anoxia, a small burst of H_2DCF oxidation was observed, induced by thiyl radicals formed during preceding hyperoxia (160 mm Hg). I_{KATP} started to oscillate after a delay with a frequency of 0.043 ± 0.002 Hz ($n = 6$; Fig. 7 A). These oscillations were accompanied by small changes of the H_2DCF oxidation rate, indicating that the cellular redox state also oscillated. When I_{KATP} became further activated, oscillations of both I_{KATP} and the H_2DCF oxidation rate ceased (Fig. 7 A). Comparison of time courses of I_{KATP} and H_2DCF oxidation during metabolic oscillations at higher time resolutions revealed that the fastest H_2DCF oxidation rate was paralleled by the highest rate of I_{KATP} activation and, vice versa, the lowest H_2DCF oxidation rate was paralleled by the highest rate of K_{ATP} channel closure (Fig. 7 B). These results suggest that at near anoxia, the ATP/ADP ratio is inversely related to the cellular redox

state, i.e., ATP synthesis is accompanied with the generation of reducing equivalents. This further suggests that ROS are not casually involved in the generation of metabolic oscillations at near anoxia.

DISCUSSION

Metabolic oscillations in isolated cardiomyocytes were observed under conditions simulating ischemia (Ryu et al., 2005; Yang et al., 2008) or reperfusion (Aon et al., 2003), but always at atmospheric oxygen. They were attributed either to oscillatory behavior of glycolysis during chemical ischemia, without obvious involvement of ROS (Yang et al., 2008), or to oxidative stress (ROS) -induced synchronization of metabolism during reperfusion (Akar et al., 2005; Aon et al., 2006). The results of the present study demonstrate that metabolic oscillations also occur in ischemic cardiomyocytes exposed to near anoxia, that they are driven by glycolysis, and that ROS are not essentially involved at this stage of ischemia. Because our experiments were performed under near-anoxic conditions, the metabolic state of a cardiomyocyte at near anoxia, in particular that of the mitochondria, is considered first.

Both glycolysis and mitochondria control the metabolic state of a cardiomyocyte at near anoxia

At normoxia, when $\Delta\Psi$ is high, ATP synthesis by the F_1F_0-ATPase decreases $\Delta\Psi$ by using the proton electrochemical potential. At near anoxia, the respiratory chain is not able to keep $\Delta\Psi$, resulting in a depolarization (Fig. 1 A). When the proton electrochemical potential, which is mainly $\Delta\Psi$, becomes lower than the free energy of the phosphorylation potential, the F_1F_0-ATPase switches from ATP synthesis to ATP hydrolysis, resulting in proton pumping. Together with the ANT, which translocates ATP^{4-} into and ADP^{3-} out of the matrix (net negative charge in), proton pumping by the F_1F_0-ATPase results in maintenance of $\Delta\Psi$ at a polarized level (Fig. 1 A). This level of $\Delta\Psi$ is maintained as long as the glycolytic ATP flux, the only source of ATP at near anoxia, supplies enough ATP to the mitochondria to keep the free energy of ATP hydrolysis below the electrochemical proton potential (Fig. 2 A). One determinant of the latter is the leak in the inner mitochondrial membrane. Because ATP^{4-} must enter the matrix against the $\Delta\Psi$ to become hydrolyzed, mitochondria that are more depolarized consume ATP at a higher rate (Fig. 4 A). Thus, ATP is hydrolyzed at the highest rate by uncoupled mitochondria (Nicholls and Ferguson, 2002).

Mitochondria are involved in metabolic oscillations at near anoxia

The results of this study demonstrate that at the beginning of I_{KATP} activation, oscillatory phenomena occur (Fig. 2 A). Because activation of I_{KATP} represents an
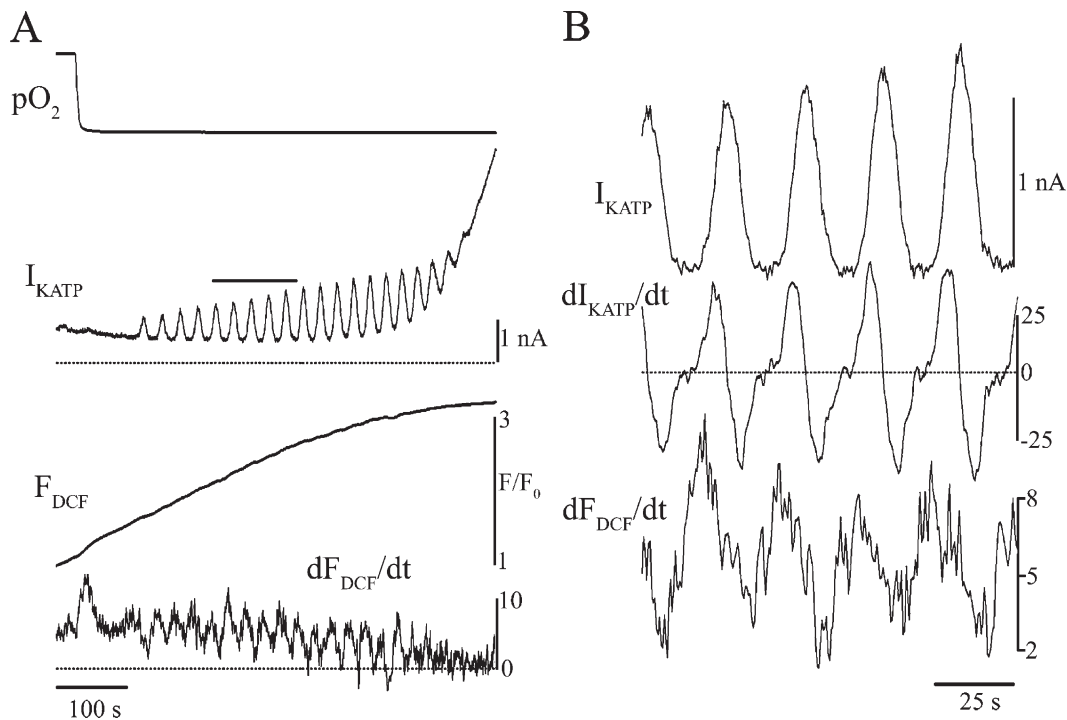
Figure 7. Redox changes during oscillatory I_{KATP} activation. (A) At near anoxia, oscillations of the H_2DCF oxidation rate occurred when I_{KATP} oscillated. (B) During oscillations at near anoxia, I_{KATP} activated at the highest rate when H_2DCF was oxidized at the highest rate. Oscillations labeled in A are shown at an extended time scale.

imbalance between the glycolytic ATP flux and ATP consumption by the F_1F_0-ATPase, oscillations of the ATP/ADP ratio can be controlled in principle at the level of both glycolysis and mitochondria. An oscillatory behavior requires a feedback. One such feedback is the link between $\Delta\Psi$ and the ATP hydrolysis rate. When the ATP concentration in the cytoplasm falls, the proton-pumping ability of the F_1F_0-ATPase decreases and $\Delta\Psi$ gets more depolarized. If the glycolytic ATP flux cannot balance this, the result would be a further ATP fall and $\Delta\Psi$ depolarization; i.e., there is a positive feedback between depolarization of $\Delta\Psi$ and the ATP consumption rate (Fig. 4 A). This positive feedback is likely to be responsible for the rapid initial ATP/ADP ratio drop with the resulting activation of I_{KATP} (Fig. 1 A). Accelerated ATP hydrolysis stimulates the glycolytic ATP flux, resulting in a slowing down of the further ATP fall (Fig. 1 A) or even transient recovery of the ATP/ADP ratio and $\Delta\Psi$ (Fig. 2 C). Hence, as long as glycolysis supplies enough ATP, the positive feedback of $\Delta\Psi$ on the ATP hydrolysis rate can be interrupted by a repetitive increase of the glycolytic ATP flux. Hence, as long as $\Delta\Psi$ oscillates, the ATP consumption rate should also oscillate, resulting in oscillations of the ATP/ADP ratio. When oscillations of $\Delta\Psi$ are small, it is likely that this feedback is of lesser significance for the control of glycolytic oscillations. Hence, it is apparently important only for the initiation of the oscillations, as it is responsible for the acceleration of the ATP/ADP ratio fall.

The other, more important positive feedback leading to oscillations of the cytoplasmic ATP/ADP ratio is driven by the effect of free ADP on the phosphofructo-kinase activity (Yang et al., 2008). In this study, metabolic oscillations were recorded at atmospheric oxygen in the presence of cyanide or rotenone, i.e., under conditions simulating ischemia at high oxygen. It was shown that in cardiomyocytes, when the capacity of oxidative phosphorylation and the creatine kinase system to buffer the cellular ATP/ADP ratio is suppressed, glycolysis could cause periodic oscillations in cellular ATP levels. As in the present study, metabolic oscillations were suppressed by IAA, persisted in cardiomyocytes pretreated with ROS scavengers, and showed an anti-phase relationship to redox oscillations (Yang et al., 2008). Notably, the frequency of metabolic oscillations in cardiomyocytes at 36°C was with 0.02–0.067 Hz, comparable to the respective frequency in our experiments at 22°C (0.044 Hz), suggesting a low Q_{10} value for the frequency-controlling process. Alternatively, the frequency-controlling process at high and low oxygen might be different.

The rate of oxygen drop affects metabolic oscillations through the rate of ATP hydrolysis

A key finding of our report is that the mitochondrial effect on metabolic oscillations depends on the speed of the oxygen drop (Fig. 5). As oxygen tension decreases, the respiratory chain slows. Hence, the speed of oxygen drop is the determinant of the rate of mitochondrial

depolarization. In turn, the $\Delta\Psi$ is a determinant of the ATP hydrolysis rate (Fig. 4 A). When the mitochondria are depolarized at a fast rate (seconds), metabolic oscillations were either elicited or potentiated (Figs. 3 and 4 B). When mitochondria are depolarized at a slow rate (minutes), the oscillatory phenomena were much less prominent because glycolysis has time to compensate for the slower fall of the ATP/ADP ratio (Fig. 5). When the blood flow is interrupted during acute ischemia in the heart, the local oxygen tension drops rapidly because oxygen is consumed by cells. Hence, the rapid (seconds) drop of oxygen in our experiments is likely to mirror acute ischemia in vivo. These results suggest that the rate of oxygen consumption in the ischemic heart is a determinant for the occurrence of glycolytic oscillations.

Lack of significant involvement of ROS and mitoK$_{ATP}$ in metabolic oscillations during early ischemia

In theory, near-anoxic conditions, i.e., highly reduced conditions, favor ROS generation by complex I of the respiratory chain (Murphy, 2009). Superoxide generated at the matrix side (Turrens, 2003; Starkov, 2008) was shown to induce permeabilization of the inner mitochondrial membrane, leading to depolarization of $\Delta\Psi$ (Echtay et al., 2002a), possibly by activating uncoupling proteins (Echtay et al., 2002b). Induction of oxidative stress did accelerate an ATP/ADP ratio drop (Fig. 6). However, at near anoxia, we did not find evidence for ROS contributing importantly at this early stage of ischemia, i.e., when $\Delta\Psi$ is still maintained by glycolysis and the respiratory chain is not noticeably damaged. Depolarization of $\Delta\Psi$ due to the opening of mitochondrial K$_{ATP}$ channels was shown to be cardioprotective (Korge et al., 2002). However, we did not observe any effects of pretreatment of cardiomyocytes with both opener and blocker of mitochondrial K$_{ATP}$ channels in our experiments. However, mitoK$_{ATP}$ channels might contribute importantly during ischemic events of longer duration and ROS during hypoxic ischemia and reperfusion (Robin et al., 2007; Korge et al., 2008).

In conclusion, we show the occurrence of glycolytic oscillations during early ischemia under near-anoxic conditions. Mitochondria affect these oscillations through the speed of ATP utilization by the backwardly running F_1F_0-ATPase, and the rate of ATP hydrolysis can be modulated by uncoupling or oxidative stress. In the ischemic heart, the speed of oxygen consumption by the tissue determines, through the speed of mitochondrial depolarization, the rate of ATP hydrolysis, which in turn determines the occurrence of oscillations in metabolism and excitability.

REFERENCES

Akar, F.G., M.A. Aon, G.F. Tomaselli, and B. O'Rourke. 2005. The mitochondrial origin of postischemic arrhythmias. *J. Clin. Invest.* 115:3527–3535. doi:10.1172/JCI25371

Aon, M.A., S. Cortassa, E. Marbán, and B. O'Rourke. 2003. Synchronized whole cell oscillations in mitochondrial metabolism triggered by a local release of reactive oxygen species in cardiac myocytes. *J. Biol. Chem.* 278:44735–44744. doi:10.1074/jbc.M302673200

Aon, M.A., S. Cortassa, and B. O'Rourke. 2006. The fundamental organization of cardiac mitochondria as a network of coupled oscillators. *Biophys. J.* 91:4317–4327. doi:10.1529/biophysj.106.087817

Aon, M.A., S. Cortassa, C. Maack, and B. O'Rourke. 2007. Sequential opening of mitochondrial ion channels as a function of glutathione redox thiol status. *J. Biol. Chem.* 282:21889–21900. doi:10.1074/jbc.M702841200

Báthori, G., G. Csordás, C. Garcia-Perez, E. Davies, and G. Hajnóczky. 2006. Ca^{2+}-dependent control of the permeability properties of the mitochondrial outer membrane and voltage-dependent anion-selective channel (VDAC). *J. Biol. Chem.* 281:17347–17358. doi:10.1074/jbc.M600906200

Bonini, M.G., C. Rota, A. Tomasi, and R.P. Mason. 2006. The oxidation of 2′,7′-dichlorofluorescin to reactive oxygen species: a self-fulfilling prophesy? *Free Radic. Biol. Med.* 40:968–975. doi:10.1016/j.freeradbiomed.2005.10.042

Brady, N.R., S.P. Elmore, J.J. van Beek, K. Krab, P.J. Courtoy, L. Hue, and H.V. Westerhoff. 2004. Coordinated behavior of mitochondria in both space and time: a reactive oxygen species-activated wave of mitochondrial depolarization. *Biophys. J.* 87:2022–2034. doi:10.1529/biophysj.103.035097

Chen, Q., S. Moghaddas, C.L. Hoppel, and E.J. Lesnefsky. 2008. Ischemic defects in the electron transport chain increase the production of reactive oxygen species from isolated rat heart mitochondria. *Am. J. Physiol. Cell Physiol.* 294:C460–C466. doi:10.1152/ajpcell.00211.2007

Dikalov, S., K.K. Griendling, and D.G. Harrison. 2007. Measurement of reactive oxygen species in cardiovascular studies. *Hypertension.* 49:717–727. doi:10.1161/01.HYP.0000258594.87211.6b

Duchen, M.R., A. Surin, and J. Jacobson. 2003. Imaging mitochondrial function in intact cells. *Methods Enzymol.* 361:353–389. doi:10.1016/S0076-6879(03)61019-0

Echtay, K.S., M.P. Murphy, R.A. Smith, D.A. Talbot, and M.D. Brand. 2002a. Superoxide activates mitochondrial uncoupling protein 2 from the matrix side. Studies using targeted antioxidants. *J. Biol. Chem.* 277:47129–47135. doi:10.1074/jbc.M208262200

Echtay, K.S., D. Roussel, J. St-Pierre, M.B. Jekabsons, S. Cadenas, J.A. Stuart, J.A. Harper, S.J. Roebuck, A. Morrison, S. Pickering, et al. 2002b. Superoxide activates mitochondrial uncoupling proteins. *Nature.* 415:96–99. doi:10.1038/415096a

Ganitkevich, V., S. Reil, B. Schwethelm, T. Schroeter, and K. Benndorf. 2006. Dynamic responses of single cardiomyocytes to graded ischemia studied by oxygen clamp in on-chip picochambers. *Circ. Res.* 99:165–171. doi:10.1161/01.RES.0000232321.89714.0e

Gnaiger, E. 2001. Bioenergetics at low oxygen: dependence of respiration and phosphorylation on oxygen and adenosine diphosphate supply. *Respir. Physiol.* 128:277–297. doi:10.1016/S0034-5687(01)00307-3

Hoffman, D.L., and P.S. Brookes. 2009. Oxygen sensitivity of mitochondrial reactive oxygen species generation depends on metabolic conditions. *J. Biol. Chem.* 284:16236–16245. doi:10.1074/jbc.M809512200

Hoffman, D.L., J.D. Salter, and P.S. Brookes. 2007. Response of mitochondrial reactive oxygen species generation to steady-state oxygen tension: implications for hypoxic cell signaling. *Am. J. Physiol. Heart Circ. Physiol.* 292:H101–H108. doi:10.1152/ajpheart .00699.2006

Korge, P., H.M. Honda, and J.N. Weiss. 2002. Protection of cardiac mitochondria by diazoxide and protein kinase C: implications for ischemic preconditioning. *Proc. Natl. Acad. Sci. USA.* 99:3312–3317. doi:10.1073/pnas.052713199

Korge, P., P. Ping, and J.N. Weiss. 2008. Reactive oxygen species production in energized cardiac mitochondria during hypoxia/reoxygenation: modulation by nitric oxide. *Circ. Res.* 103:873–880. doi:10.1161/CIRCRESAHA.108.180869

Leyssens, A., A.V. Nowicky, L. Patterson, M. Crompton, and M.R. Duchen. 1996. The relationship between mitochondrial state, ATP hydrolysis, $[Mg^{2+}]_i$ and $[Ca^{2+}]_i$ studied in isolated rat cardiomyocytes. *J. Physiol.* 496:111–128.

Marchesi, E., C. Rota, Y.C. Fann, C.F. Chignell, and R.P. Mason. 1999. Photoreduction of the fluorescent dye 2′-7′-dichlorofluorescein: a spin trapping and direct electron spin resonance study with implications for oxidative stress measurements. *Free Radic. Biol. Med.* 26:148–161. doi:10.1016/S0891-5849(98)00174-9

Muller, F.L. 2009. A critical evaluation of cpYFP as a probe for superoxide. *Free Radic. Biol. Med.* 47:1779–1780. doi:10.1016/j.freeradbiomed.2009.09.019

Murphy, M.P. 2009. How mitochondria produce reactive oxygen species. *Biochem. J.* 417:1–13. doi:10.1042/BJ20081386

Nicholls, D.G., and S.J. Ferguson. 2002. Bioenergetics. Academic Press, London. 297 pp.

Nicholls, D.G., and M.W. Ward. 2000. Mitochondrial membrane potential and neuronal glutamate excitotoxicity: mortality and millivolts. *Trends Neurosci.* 23:166–174. doi:10.1016/S0166-2236(99)01534-9

O'Neill, P., and P. Wardman. 2009. Radiation chemistry comes before radiation biology. *Int. J. Radiat. Biol.* 85:9–25. doi:10.1080/09553000802640401

O'Rourke, B., B.M. Ramza, and E. Marban. 1994. Oscillations of membrane current and excitability driven by metabolic oscillations in heart cells. *Science.* 265:962–966. doi:10.1126/science.8052856

Robin, E., R.D. Guzy, G. Loor, H. Iwase, G.B. Waypa, J.D. Marks, T.L. Hoek, and P.T. Schumacker. 2007. Oxidant stress during simulated ischemia primes cardiomyocytes for cell death during reperfusion. *J. Biol. Chem.* 282:19133–19143. doi:10.1074/jbc.M701917200

Romashko, D.N., E. Marban, and B. O'Rourke. 1998. Subcellular metabolic transients and mitochondrial redox waves in heart cells. *Proc. Natl. Acad. Sci. USA.* 95:1618–1623. doi:10.1073/pnas.95.4.1618

Rota, C., C.F. Chignell, and R.P. Mason. 1999a. Evidence for free radical formation during the oxidation of 2′-7′-dichlorofluorescin to the fluorescent dye 2′-7′-dichlorofluorescein by horseradish peroxidase: possible implications for oxidative stress measurements. *Free Radic. Biol. Med.* 27:873–881. doi:10.1016/S0891-5849(99)00137-9

Rota, C., Y.C. Fann, and R.P. Mason. 1999b. Phenoxyl free radical formation during the oxidation of the fluorescent dye 2′,7′-dichlorofluorescein by horseradish peroxidase. Possible consequences for oxidative stress measurements. *J. Biol. Chem.* 274:28161–28168. doi:10.1074/jbc.274.40.28161

Rumsey, W.L., C. Schlosser, E.M. Nuutinen, M. Robiolio, and D.F. Wilson. 1990. Cellular energetics and the oxygen dependence of respiration in cardiac myocytes isolated from adult rat. *J. Biol. Chem.* 265:15392–15402.

Ryu, S.Y., S.H. Lee, and W.K. Ho. 2005. Generation of metabolic oscillations by mitoKATP and ATP synthase during simulated ischemia in ventricular myocytes. *J. Mol. Cell. Cardiol.* 39:874–881. doi:10.1016/j.yjmcc.2005.08.011

Slodzinski, M.K., M.A. Aon, and B. O'Rourke. 2008. Glutathione oxidation as a trigger of mitochondrial depolarization and oscillation in intact hearts. *J. Mol. Cell. Cardiol.* 45:650–660. doi:10.1016/j.yjmcc.2008.07.017

Starkov, A.A. 2008. The role of mitochondria in reactive oxygen species metabolism and signaling. *Ann. NY Acad. Sci.* 1147:37–52.

Stowe, D.F., and A.K.S. Camara. 2009. Mitochondrial reactive oxygen species production in excitable cells: modulators of mitochondrial and cell function. *Antioxid. Redox Signal.* 11:1373–1414. doi:10.1089/ars.2008.2331

Turrens, J.F. 2003. Mitochondrial formation of reactive oxygen species. *J. Physiol.* 552:335–344. doi:10.1113/jphysiol.2003.049478

Voronina, S.G., S.L. Barrow, O.V. Gerasimenko, O.H. Petersen, and A.V. Tepikin. 2004. Effects of secretagogues and bile acids on mitochondrial membrane potential of pancreatic acinar cells: comparison of different modes of evaluating DeltaPsim. *J. Biol. Chem.* 279:27327–27338. doi:10.1074/jbc.M311698200

Wardman, P. 2007. Fluorescent and luminescent probes for measurement of oxidative and nitrosative species in cells and tissues: progress, pitfalls, and prospects. *Free Radic. Biol. Med.* 43:995–1022. doi:10.1016/j.freeradbiomed.2007.06.026

Wilson, D.F., W.L. Rumsey, T.J. Green, and J.M. Vanderkooi. 1988. The oxygen dependence of mitochondrial oxidative phosphorylation measured by a new optical method for measuring oxygen concentration. *J. Biol. Chem.* 263:2712–2718.

Winterbourn, C.C. 1993. Superoxide as an intracellular radical sink. *Free Radic. Biol. Med.* 14:85–90. doi:10.1016/0891-5849(93)90512-S

Winterbourn, C.C. 2008. Reconciling the chemistry and biology of reactive oxygen species. *Nat. Chem. Biol.* 4:278–286. doi:10.1038/nchembio.85

Winterbourn, C.C., and M.B. Hampton. 2008. Thiol chemistry and specificity in redox signaling. *Free Radic. Biol. Med.* 45:549–561. doi:10.1016/j.freeradbiomed.2008.05.004

Wrona, M., K.B. Patel, and P. Wardman. 2008. The roles of thiol-derived radicals in the use of 2′,7′-dichlorodihydrofluorescein as a probe for oxidative stress. *Free Radic. Biol. Med.* 44:56–62. doi:10.1016/j.freeradbiomed.2007.09.005

Yang, J.H., L. Yang, Z. Qu, and J.N. Weiss. 2008. Glycolytic oscillations in isolated rabbit ventricular myocytes. *J. Biol. Chem.* 283:36321–36327. doi:10.1074/jbc.M804794200

Yellon, D.M., and D.J. Hausenloy. 2007. Myocardial reperfusion injury. *N. Engl. J. Med.* 357:1121–1135. doi:10.1056/NEJMra071667

Zorov, D.B., C.R. Filburn, L.O. Klotz, J.L. Zweier, and S.J. Sollott. 2000. Reactive oxygen species (ROS)-induced ROS release: a new phenomenon accompanying induction of the mitochondrial permeability transition in cardiac myocytes. *J. Exp. Med.* 192:1001–1014. doi:10.1084/jem.192.7.1001